Plant Physiol. (1991) 95, 305–315
0032-0889/91/95/0305/11/$01.00/0

Received for publication August 10, 1990
Accepted October 3, 1990

Water Transport across Maize Roots[1]

Simultaneous Measurement of Flows at the Cell and Root Level by Double Pressure Probe Technique

Guo Li Zhu and Ernst Steudle*

Lehrstuhl für Pflanzenökologie, Universität Bayreuth, Universitätsstrasse 30, D-8580 Bayreuth, Federal Republic of Germany

ABSTRACT

A double pressure probe technique was used to measure simultaneously water flows and hydraulic parameters of individual cells and of excised roots of young seedlings of maize (*Zea mays* L.) in osmotic experiments. By following initial flows of water at the cell and root level and by estimating the profiles of driving forces (water potentials) across the root, the hydraulic conductivity of individual cell layers was evaluated. Since the hydraulic conductivity of the cell-to-cell path was determined separately, the hydraulic conductivity of the cell wall material could be evaluated as well (Lp_{cw} = 0.3 to $6 \cdot 10^{-9}$ per meter per second per megapascal). Although, for radial water flow across the cortex and rhizodermis, the apoplasmic path was predominant, the contribution of the hydraulic conductance of the cell-to-cell path to the overall conductance increased significantly from the first layer of the cortex toward the inner layers from 2% to 23%. This change was mainly due to an increase of the hydraulic conductivity of the cell membranes which was $Lp = 1.9 \cdot 10^{-7}$ per meter per second per megapascal in the first layer and Lp = 14 to $9 \cdot 10^{-7}$ per meter per second per megapascal in the inner layers of the cortex. The hydraulic conductivity of entire roots depended on whether hydrostatic or osmotic forces were used to induce water flows. Hydrostatic Lp_r was 1.2 to $2.3 \cdot 10^{-7}$ per meter per second per megapascal and osmotic Lp_r = 1.6 to $2.8 \cdot 10^{-8}$ per meter per second per megapascal. The apparent reflection coefficients of root cells (σ_s) of nonpermeating solutes (KCl, PEG 6000) decreased from values close to unity in the rhizodermis to about 0.7 to 0.8 in the cortex. In all cases, however, σ_s was significantly larger than the reflection coefficient of entire roots (σ_{sr}). For KCl and PEG 6000, σ_{sr} was 0.53 and 0.64, respectively. The results are discussed in terms of a composite membrane model of the root.

The modeling of water flows across roots receives great interest, because the hydraulic resistance of the root is an important physiological and ecological parameter. Usually, it is thought that in the cortex the flow of water is apoplasmic (*i.e.* around cells) up to the Casparian band which requires a membrane-bound transport step across the endodermis. In the stele and up the vessels, flow should be then again in the apoplast. In transpiring plants, the radial flow of water across the root will be driven by hydrostatic forces set up by the tension in the vessel. However, under conditions of low or zero transpiration, the forces will be mainly osmotic and water flow will be coupled to the osmotic gradient set up by the active accumulation of nutrients in the root xylem. Under these conditions, positive pressures are built up in the xylem.

Most of the current models of water transport imply that roots behave like osmometers, *i.e.* an interior (xylem) and the medium are separated by a membrane-like structure (3, 4, 10, 12, 15, 17–20). Alternatively, more complex models have been developed that include several barriers in the root cylinder arranged in series (*e.g.* ref. 11) and also the longitudinal transport in the xylem (6). Taura *et al.* (22) have proposed that in such models the coupling between active uptake of nutrients and water flow will be the governing component even in the transpiring plant. Although the role of the endodermis as a substantial barrier is not questioned in these models, there is some debate of whether the exodermis could be an additional barrier of comparable importance. The work of Peterson (13) indicates that the exodermis could effectively exclude hydrophilic substances from the cortex, whereas other people (2) think that this structure is fairly permeable.

The root pressure probe has been used to work out the water and solute permeability of roots (6, 15, 17–20). These data have been compared with those obtained at the cell level (by the conventional cell pressure probe; 8) to evaluate the relative importance of pathways. For some species (barley, bean), the results indicated a considerable cell-to-cell component, whereas in others (maize) the apoplast seemed to be preferred. However, the relative contribution of pathways also depended on the nature of the forces applied. In osmotic experiments, the cell-to-cell path was preferred, whereas in hydrostatic experiments the flow was predominantly in the apoplast. The results also indicated a considerable apoplasmic by-pass of water in the endodermis. In addition, for all species, the reflection coefficients of roots (σ_{sr}) (Table I) were substantially lower than unity even for solutes for which cell membranes exhibit a $\sigma_s \approx 1$. These findings have been interpreted by an extended osmometer model in which the osmotic barrier in the root is looked at as a composite membrane system (15, 17, 18, 20).

In the earlier experiments, the measurements at the cell and root level have been performed separately, *i.e.* by using the two different types of probes on different roots. However, it would be desirable to follow the flows simultaneously at the

[1] This work was supported by a grant from the Deutsche Forschungsgemeinschaft, Sonderforschungsbereich 137.

Table I. *Abbreviations Used in This Paper*

A	cell surface area
A_r	surface area of root
A_r^j	area of layer j of cortex
V and V_s	cell volume of cortical and stelar cells
V_x	volume of xylem
d	cell diameter
l	cell length
r_o	radius of root
r_j	radius of layer j of cortex
γ_{cc} and γ_{cw}	fractional contribution of the cell-to-cell and cell wall pathway to the total cross-sectional area
P	cell turgor pressure
P_o	cell turgor pressure before osmotic treatment
P_{min}	new equilibrium cell turgor pressure in osmotic treatment
P_r	root pressure
k_s	rate constant of solute exchange
k_w and k_{rw}	rate constant of water exchange of cells and roots
$T_{½}$ and $T_{r½}$	half-time of water exchange of cells and roots
Lp	hydraulic conductivity of cell membrane
Lp_{cw}	hydraulic conductivity of cell wall material
L_j	hydraulic conductivity of layer j of cortex
Lp_{cor}	hydraulic conductivity of cortex
Lp_r	hydraulic conductivity of root
ϵ	elastic modulus of cell
ϵ_x	elastic modulus of xylem
σ_s	reflection coefficient of cell
σ_{sr}	reflection coefficient of root
ψ_j	water potential of layer j of cortex
ψ_{m1}	water potential in root medium before osmotic treatment
ψ_{m2}	water potential in root medium during osmotic treatment
ψ_v	water potential of cell vacuole
π^i	osmotic pressure of cell
n_j	number of cells in layer j of cortex
Φ_j	radial flow of water across layer j in $m^3 \cdot s^{-1}$
J_j	density of radial flow of water across layer j in $m^3 \cdot m^{-2} \cdot s^{-1}$

cell and root level in order to get a more detailed picture. In the present paper, experiments of this type are described which yield transient profiles of water flow and water potential in the root as well as information about the hydraulic conductance of the apoplasmic and cell-to-cell pathways. Here, we describe initial water flows in roots at the cell and entire root level resulting from an osmotic treatment. A more rigorous description of the processes, i.e. of the propagation of changes of water potential across roots, will be given in a subsequent paper.

MATERIALS AND METHODS

Plant Material

Maize seeds (*Zea mays* L. cv 'Tanker'; Südwestdeutsche Saatzucht, Rastatt, FRG) were germinated in the dark for 2 to 3 d at 25°C on wet filter paper. When the seminal roots of the seedlings were 30 to 50 mm long, they were transferred to plastic tanks (6 L) with aerated one-half Miller solution (see ref. 6) for 8 to 11 d in a growing chamber [macronutrients in mM: K_2HPO_4, 0.8; $(NH_4)_2SO_4$, 0.8; $Ca(NO_3)_2$, 0.8; $Mg(NO_3)_2$, 1; NH_4NO_3, 0.5; micronutrients in μM: Cl^-, 50; BO_3^{3-}, 25; Mn^{2+}, 2; Zn^{2+}, 2; Cu^{2+}, 0.5; MoO_4^{2-}, 0.5; NaFeEDTA, 36 (pH 6); total osmolarity, 8–10 mOsmol]. The light/dark regime was 12/12 h and the temperature 22/19°C. Photosynthetic photon flux density was 300 $\mu mol \cdot m^{-2} \cdot s^{-1}$. Main roots were 150 to 250 mm long with a diameter of 0.8 to 1.2 mm from which end segments of a length of 75 mm were cut for the experiments. Average dimensions of rhizodermis and cortex cells were determined from photographs of freehand cross and longitudinal sections at distances of 40, 50, 60, and 70 mm from the root tip. Surface areas of cortical cell layers (A_r^j) and of the root surface area (A_r) were estimated from the diameters of the appropriate cylinders (2 r_o and 2 r_j) formed by these layers and from the length of the root segments.

Root Pressure Probe Measurements

As shown in Figure 1, an end segment of a root was tightly connected to a root pressure probe (17–20). The seal used to fix the root was prepared from liquid silicone material (Xantopren plus from Bayer, Leverkusen, FRG). The length of the seal was 8 mm to ensure a large area of sealing without interrupting xylem vessels. Appropriate sealing was checked after each experiment by cutting the root right at the seal. Roots were inserted into a glass tube with an inner diameter of 3 mm, through which the medium was pumped to ensure sufficient stirring of the solution. The time for the exchange of solution in the tube was less than 1 s which was much smaller than the time constants of the processes observed. The glass tube was fixed on the sample holder plate of a stereomicroscope (Wild M 420, Switzerland). Roots were fixed in the glass tube by small holders prepared from stainless steel wire (0.4 mm in diameter) to avoid vibrations of the root

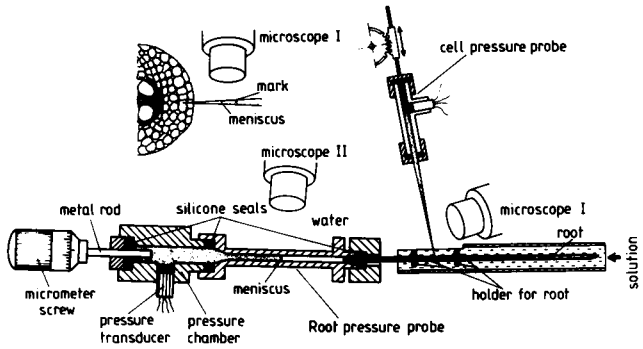

Figure 1. Experimental set-up for the simultaneous measurement of water and solute transport parameters of excised roots and of single cortical cells. Measurements at the root level were performed using the root pressure probe. At the level of individual cells, the cell pressure probe was employed. Parameters could be measured by either changing the root and cell turgor pressures (hydrostatic experiments) or by changing the osmotic pressure of the medium (osmotic experiments) and following the subsequent adjustment of water potential in cells and in the root xylem. (For further explanation, see text.)

caused by the flow of solution. The fixed part of the root was viewed by the stereomicroscope (magnification ×160).

Cell Pressure Probe Measurements

A cell pressure probe was arranged at a right angle to the root (Fig. 1) and was used to determine hydraulic parameters (elastic modulus: ϵ; half-time of water exchange: $T_{1/2}$; and hydraulic conductivity: Lp; 8, 15, 19–21). Both pressure probes were mounted on micromanipulators (Leitz) and were operated simultaneously. The glass microcapillaries used in the cell pressure probe had external diameters of 1 mm. They were pulled on an upright puller to a diameter of about 1 μm. They were filled with silicone oil. Prior to the experiments, the tips of the microcapillaries were broken with the aid of the micromanipulator under the microscope by gently touching an upright surface to yield final tip diameters of 3 to 5 μm. No bevelling of the tips was necessary in the experiments with maize cortical cells. Microcapillaries were marked about 100 μm behind the tip with water-insoluble ink to estimate the distance of the tip within the root and the cell layer punctured by the pressure probe using the measured dimensions of cortex cells (see above).

Experimental Procedure

When the root was arranged in the way described above and the root pressure had attained a stationary level (P_{ro}), the root pressure probe was used to determine the hydraulic parameters ($T_{r1/2}$, Lp_r) in hydrostatic experiments (17–20). Then the microcapillary of the cell pressure probe was pushed into a cortical cell. When the turgor pressure became constant, hydraulic parameters of the cell were determined (P_o, ϵ, $T_{1/2}$, Lp; 19–21). Then the bathing medium (one-half Miller solution) of the root was exchanged for the test solution (one-half Miller solution + osmoticum), and the exosmotic relaxation process of the root and the cell turgor pressure were measured simultaneously. When the root and cell turgor pressure had reached new steady levels in the presence of a test solute, the medium was changed back to the original solution. Again, the responses of the root and the cell turgor pressure were recorded until water flow equilibrium was attained. Lp_r was calculated from the rate constant k_{rw} of the process, i.e. Steudle *et al.* (20):

$$k_{rw} = A_r \cdot Lp_r \cdot (\Delta P_r / \Delta V_{app}). \tag{1}$$

k_{rw} is related to the half-time $T_{r1/2}$ ($k_{rw} = \ln(2)/T_{r1/2}$). A_r = surface area of the root. $\Delta P_r/\Delta V_{app}$ is a measure of the elasticity of the root pressure probe (change in root pressure (ΔP_r) measured in response to a change in volume (ΔV_{app})). Cell Lp was estimated from Equation 2:

$$Lp = \frac{V \cdot \ln(2)}{A \cdot T_{1/2}(\epsilon + \pi^i)} = \frac{\ln(2)}{A \cdot T_{1/2}(dP/dV + \pi^i/V)} = \frac{\ln(2)}{T_{1/2}(\pi dl \cdot dP/dV + 4/d \cdot \pi^i)}. \tag{2}$$

Here, $V = \pi \cdot l \cdot d^2/4$ = volume of cyclindrical cell, $A = \pi \cdot d \cdot l$ = surface area of cyclindrical cell ($l \gg d/2$); $T_{1/2}$ = half time of water exchange. $\epsilon = V\,dP/dV$ = elastic modulus of cell and $dP/dV \approx \Delta P/\Delta V$ is the change in pressure measured in the system per change in volume; π^i = osmotic pressure in the vacuole of cell; $k_w = \ln(2)/T_{1/2}$ (8, 19–21). π^i was obtained from the stationary cell turgor (P_o) and from the osmotic pressure of the medium (π^o) at water flow equilibrium prior to the experiment, since $\pi^i = P_o + \pi^o$. This estimation of π^i assumes a reflection coefficient of unity of the solutes in the cell and in the nutrient medium and, could, therefore, underestimate π^i. On the other hand, if $\sigma_s < 1$, a more rigorous derivation of Equation 2 would show that $\sigma_s \cdot \pi^i$ would have to be used instead of π^i. Thus, the value estimated is the appropriate one. Both, the apparent reflection coefficient of cells (σ_s) and roots (σ_{sr}) were calculated from earlier work by Steudle and coworkers (15, 17, 18, 20):

$$\sigma = \frac{\Delta P}{\Delta \pi^o} \frac{\epsilon + \pi^i}{\epsilon} \exp(k_s \cdot t_{min}). \tag{3}$$

Here, $\Delta P = P_o - P_{min}$ is the maximum change in root or cell turgor pressure measured in response to a change of the osmotic pressure of the medium ($\Delta\pi^o$). P_o = original root or cell turgor pressure before osmotic experiments; P_{min} = minimum root or cell turgor pressure; ϵ = elastic modulus of xylem (ϵ_x) or cells (ϵ). The factor of $(\epsilon + \pi^i)/\epsilon$ is correcting for concentration changes in the xylem or cells, respectively, induced by volume changes. The exponential term corrects for passive solute flow (k_s = rate constant of solute exchange; t_{min} = time required to reach P_{min}; 15, 20). For both, cells and entire roots, this factor was assumed to be unity for the solutes used (KCl and PEG 6000).

Changes in root and cell turgor pressure with time (t) during osmotic shrinking or swelling were described earlier (8, 21, 23):

$$P = (P_o - P_{min}) \exp(-k \cdot t) + P_{min}. \tag{4}$$

k is the rate constant for water exchange for roots (k_{rw}) or for cells (k_w).

Calculation of Profiles of Initial Water Flows and of Water Potentials Across the Root Cortex

An end segment of a root is considered which comprises a tip part with immature xylem (about 15 mm in length; 6), and the main part of a length of about 60 mm in which measurements of root pressure were performed. From double pressure probe experiments, the net flow of water from each layer of the cortex to the medium can be estimated as well as the efflux of water from the xylem following an increase of the osmotic pressure of the medium. For a cell it is valid that:

$$\frac{dV}{dt} = \frac{dV}{dP}\frac{dP}{dt} = \frac{V}{\epsilon}\frac{dP}{dt}, \qquad (\epsilon \equiv V \cdot dP/dV) \tag{5}$$

and for a root:

$$\frac{dV_r}{dt} = \frac{dV_{app}}{dP_r}\frac{dP_r}{dt}. \tag{6}$$

Thus, dP/dV ($\approx \Delta P/\Delta V$) and dP_r/dV_{app} ($\approx \Delta P_r/\Delta V_{app}$) are measured with the cell and root pressure probe, respectively, to convert changes in turgor pressure into changes in cell volume (*i.e.* into rates of cell shrinking) and into a radial flow of water across the root.

Provided that the radial flow of water across the root is quasi-steady at each point during the initial period of time (*i.e.* during the first 10–20 s), estimates of the profiles of water potential (ψ) and the water flow (Φ in $m^3 \cdot s^{-1}$) can be made. From these estimations, conclusions can be drawn about the relative importance of the cell-to-cell and apoplasmic pathways for water in the cortex.

It is valid that during an osmotic treatment both, the root protoplasts and the apoplast should shrink at any position in the root. At least, they should not enlarge. Therefore, for any cell layer of the cylindrical root starting with the first (rhizodermal) layer ($j = 0$), the total initial flow of water crossing this layer ($\Phi_j(t = 0)$ in $m^3 \cdot s^{-1}$) can be given, *i.e.*:

$$\Phi_j(t=0) = \sum_{i=9}^{j} n_i \left(\frac{dV}{dt}\right)_{t=0} + \sum_{i=10}^{n} n_i \left(\frac{dV_s}{dt}\right)_{t=0} + \left(\frac{dV_x}{dt}\right)_{t=0}, \quad (7)$$

where $0 \leq j < 9$ and $n > 9$. In Equation 7, nine layers of cortical cells (cell volume = V) are considered with varying amounts of n_j cells in each layer as well as stelar cells (cell volume = V_s). The last term on the right side denotes the contribution of the water flow out of the xylem. Initial changes of cell volumes with time (t) are directly obtained from the measured changes in turgor, since from Equation 5:

$$\left(\frac{dV}{dt}\right)_{t=0} = \frac{dV}{dP} \cdot \left(\frac{dP}{dt}\right)_{t=0}. \quad (8)$$

The numbers of cells in different layers (n_j) are obtained from cross and longitudinal sections of roots (see above).

In Equation 7, the contribution of the wall compartment to the overall shrinking of the tissue has been neglected. From the measurements of the amounts of shrinking of cells and xylem, it can be verified that during the initial phase the contribution of the stelar cells and of xylem to the overall movement of water should be fairly small. Thus, it is reasonable to also neglect these contributions and to evaluate flows from the shrinking of the cortex only. The radial flow of water per unit area of cell layer (J_j) will be:

$$J_j = \Phi_j / A_r^j. \quad (9)$$

A_r^j = surface area of layer j. Thus, for the cortex, the profiles of initial water flow can be also given in units of $m^3 \cdot m^{-2} \cdot s^{-1}$.

Hydraulic Conductance of Cell-to-Cell and Apoplasmic Pathways

Under steady conditions, the flows given in Equation 9 are related to driving forces (differences in water potential across the layers, $\Delta\psi_j$) and to hydraulic conductances of the layers, $L_j \cdot A_r^j$ (L_j = hydraulic conductivity of layer j):

$$\frac{1}{L_j} J_j = \frac{\Phi_j}{L_j \cdot A_r^j} = \Delta\Psi_j. \quad (10)$$

This equation assumes that, within the tissue, the driving forces are matric or hydrostatic in nature rather than osmotic. Otherwise, the reflection coefficients of the layers would have to be introduced. In Equation 10, the latter parameters are incorporated in the L_j. The hydraulic conductivity of a cell layer (L_j) is related to the conductivities of the parallel cell-to-cell and apoplasmic paths by:

$$L_j = \gamma_{cc} \frac{Lp_j}{2} + \gamma_{cw} \frac{Lp_{cwj}}{d_j}, \quad (11)$$

where γ_{cc} and γ_{cw} are the fractional contributions of the cell-to-cell and cell wall pathways to the total cross-sectional area ($\gamma_{cc} + \gamma_{cw} = 1$). The factor of two in the term for the cell-to-cell component in Equation 11 denotes the fact that the cell membrane has to be crossed twice per cell layer. Lp_{cw} is the hydraulic conductivity of the cell wall material in $m^2 \cdot s^{-1} \cdot MPa^{-1}$ and d the diameter of a layer.

Equation 10 was used to evaluate the hydraulic conductivity (L_j) of cell layers. The roots were first equilibrated in the root medium prior to a change in the water potential of the medium (ψ_{m1}). After the change, they tended to attain the new equilibrium water potential (ψ_{m2}). During the initial phase of this process, changes of ψ in layers deeper than the cortex were fairly small and water flows coming from the stele and xylem were neglected (see above and also "Discussion"). To a good approximation, the entire water potential applied dropped across the cortex during this phase. In order to work out the drop in water potential across individual cell layers ($\Delta\psi_j$), it was assumed that the water potential difference driving the initial flow out of a cell in a certain layer j was the difference between the water potential in the vacuole (ψ_{vj}) and the mean of the water potentials at the inner (ψ_{j+}) and outer (ψ_{j-}) tangential walls. Thus, the initial water flow from a cell of this layer will be given by:

$$\left(\frac{dV_j}{dt}\right)_{t=0} = Lp_j \cdot A_j \cdot \left(\psi_{vj} - \frac{\psi_{j+} + \psi_{j-}}{2}\right). \quad (12)$$

At $t = 0$, ψ_{vj} and the ψ_{j+} of the last cortical layer will be still at the original water potential before the change and, therefore, the ψ_{j-} of this layer can be evaluated. Thus, by measuring $(dV/dt)_{t=0}$ for layers 9 to 0 (Rh) and also knowing Lp and A, the ψ_j values of the layers can be successively evaluated, and the values of $\Delta\psi_j$ can be calculated for all layers. This procedure of successively evaluating $\Delta\psi_j$ had to be used instead of summing up the drops across individual layers because the L_j were not constant.

Since $\Delta\psi_j$, Φ_j, and A_r^j are known, the hydraulic conductivities of individual cell layers (L_j) can be also calculated (Equation 10). Furthermore, Equation 11 can be applied to evaluate Lp_{cw} (hydraulic conductivity of cell wall material) and the ratio between the hydraulic conductances of protoplasts and apoplast across a layer (ρ_j) by:

$$\rho_j = \frac{\gamma_{cc} \cdot Lp_j \cdot d_j}{2 \cdot \gamma_{cw} \cdot Lp_{cw}}. \quad (13)$$

The hydraulic conductivity of the entire cortex (per m^2 of outer root surface area) will be:

$$\frac{1}{Lp_{cor}} = \sum_{j=o}^{9} \frac{1}{L_j} \cdot \frac{r_o}{r_j}. \quad (14)$$

r_o = radius of root; r_j = radius of layer j; $j = 0$ denotes the rhizodermis. This value of Lp_{cor} could be compared with the

Lp_r measured for the entire root in hydrostatic and osmotic root pressure relaxation experiments (see "Discussion").

RESULTS

Cell Dimensions and Cell Numbers in Maize Roots

Measurements of cell dimensions and numbers were performed using root sections in a range between 40 and 70 mm from the root apex, *i.e.* in a range where the cell pressure probe was also used. In this range, the diameters of the cells in the cortex were fairly uniform (Table II). Diameters of rhizodermis cells were about half of that of the cortex. In the range between 40 and 75 mm, there was a slight tendency for the cells to become shorter toward the apex (as one would expect), but these differences were not significant (data not shown). Therefore, an average value was calculated for the cell length (l in Table II). In different layers, the numbers of cells increased from inside of the root to the surface, being 35 cells in layer 9 and 150 cells in the rhizodermis. The total number of rhizodermis and cortex cells in the range between 40 and 75 mm from the apex was about $1.5 \cdot 10^5$.

Water Relation Parameters and Reflection Coefficients of Cortex Cells and of Roots

A typical experiment for the determination of water relation parameters using the double pressure probe is shown in Figure 2. On the left side of the figure, hydrostatic determination of hydraulic parameters are shown for the cell (A) and the root (B) level. On the right side, osmotic responses are given using KCl as the osmotic solute. In the experiment shown in the figure, the cell was close to the root surface (rhizodermis). It can be seen that the half time of water exchange of the cell was much smaller than that of the root for both exosmotic and endosmotic changes. The response in cell turgor pressure to a change of the osmotic pressure of the medium differed markedly from that in root pressure. This led to different

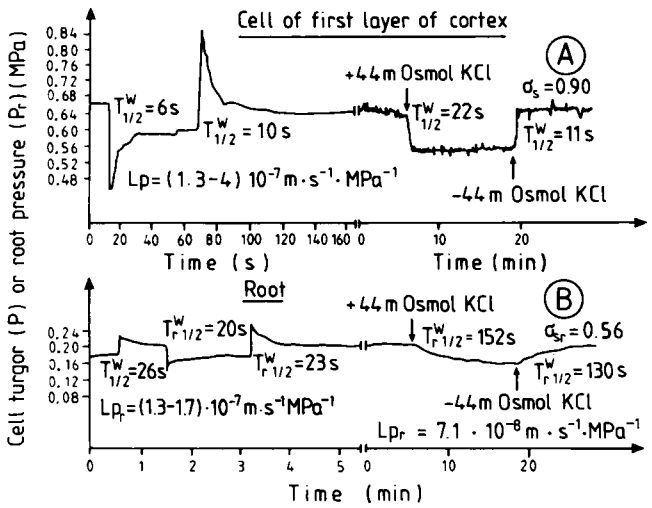

Figure 2. Typical examples of simultaneous measurements at the cell and root level (A, cell level; B, root level). First, hydraulic parameters (hydraulic conductivity of cell membranes [Lp] and of roots [Lp_r]; half-time of water exchange of cells [$T_{½}$] and of roots [$T_{r½}$]) were determined hydrostatically at both levels left parts of traces A and B. Then, with the tip of the cell pressure probe still staying in the cell, the osmotic pressure of the root medium was changed, and the responses in the pressures in the cell and in the root xylem were recorded (right side of curves of A and B). When the cell turgor and root pressure had attained a new equilibrium level, the root medium which contained the test solute (KCl) was changed back to the original solution. For each run, the half-times of osmotic responses were measured.

Table II. *Cell Numbers and Geometry of Cortex Cells*

The dimensions and numbers of cortex cells (mean ± SD) in root segments (between 40 and 75 mm from the apex). Values are the average of observations taken from longitudinal and cross-sections at 40, 50, 60, and 70 mm behind the root tip. The total cell number refers to the entire length of the segments. For each value, the number of observations was not smaller than 20.

Layer	Cell Diameter (d)	Cell Length (l)	Number of Cells in Cross-section	Total Number of Cortex Cells
		μm		
Rh	21 ± 6		147 ± 14	
1st	35 ± 8		80 ± 19	
2nd	36 ± 7		73 ± 12	
3rd	41 ± 9		57 ± 15	
4th	45 ± 11		51 ± 5	
5th	43 ± 5	150 ± 46	49 ± 7	1.5×10^5
6th	45 ± 9		45 ± 5	
7th	34 ± 6		48 ± 6	
8th	36 ± 5		41 ± 4	
9th	33 ± 7		34 ± 7	

reflection coefficients for the cell ($\sigma_s = 0.90$) and for the root ($\sigma_{sr} = 0.56$).

The half time of the response of cortex cells to osmotic changes of the medium markedly increased with increasing distance from the root surface. For the innermost layer of the cortex $T_{½}$ was close to $T_{r½}$ (Fig. 3). This means that the rate of the response became smaller in the same direction (*i.e.* $[dP/dt]_{t=0}$ became smaller). In the deeper layers, the differences between the layers were not as clear as at the root surface. Therefore, the data given in Figure 3 for hydraulic parameters of cortical cells are grouped (layers 3–4, 5–6, and 7–9, respectively). The reflection coefficients of cells of the rhizodermis were higher than that of deeper cells, although $\sigma_s > \sigma_{sr}$ was valid for all layers.

Table III summarizes all results obtained at the cell and root level by the double pressure probe technique. Part A of the table indicates that the hydraulic properties of the cortex cells were not homogeneous. $T_{½}$ decreased toward the stele. Statistically, the slight increase from layers 5 and 6 to layers 7 to 9 was not significant. Instead of the elastic modulus of the cell (ϵ), the directly measured 'elasticity of the system,' dP/dV, is given in Table III, A. This value has been used to calculate Lp and initial water flows according to Equations 2, 5, and 8. It can be seen that dP/dV remained fairly constant. Since dP/dV could be determined with the pressure probe with high accuracy (see below), the variations in dP/dV shown in the table reflect differences between cells. ϵ values ranged between $\epsilon = 1.7$ MPa for epidermal cells and $\epsilon = 1.9$ to 4.3

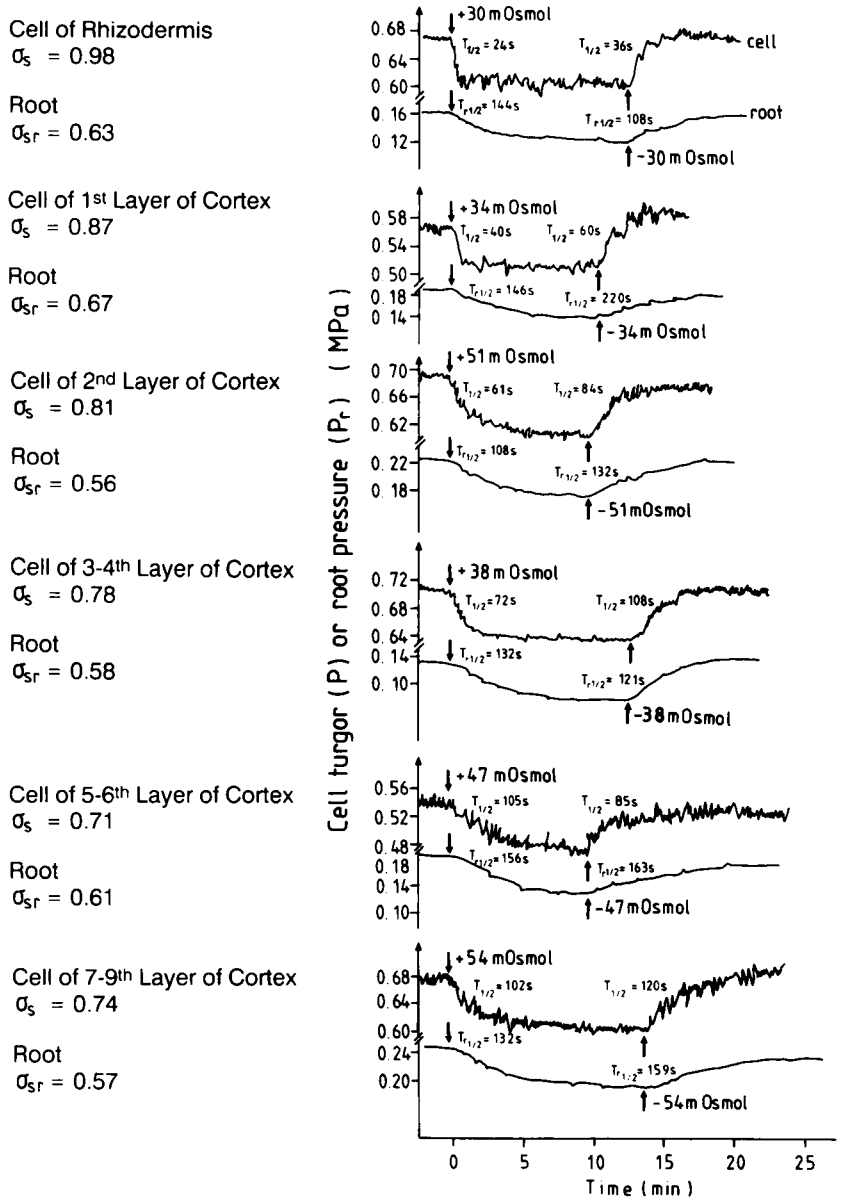

Figure 3. Dependence of the response in cell turgor of cortical cells to changes of the osmotic pressure of the medium on the position of the cells in the cortex (osmoticum: PEG 6000). For each position (rhizodermis and layers 1, 2, 3–4, 5–6, and 7–9), responses of the entire root are given as well. Traces are from two different roots (first root: rhizodermis to layer 2; second root: layers 3–4 to 7–9).

MPa for cortical cells. Thus, ϵ also remained fairly constant and the changes in $T_{1/2}$ were due to an increase of the hydraulic conductivity of the cell membrane (Lp). It has to be noted that, in principle, the measured value of Lp should represent the hydraulic conductivity of a pathway of water movement from the vacuole to a background 'reservoir' somewhere in the vicinity of the cell or protoplast. It should also incorporate apoplasmic components. However, these components should hardly affect the absolute value of the conductivity of the entire barrier, since the amount of water exchanged between protoplast and surroundings is fairly small and the hydraulic conductivity of the wall material is high (see below and "Discussion"). It can be seen from part A of Table III that the hydraulic conductivity of the entire root (from hydrostatic experiments) was of the same order of magnitude as the cell Lp of the outer cell layer, but Lp_r from hydrostatic experiments was by a factor of 6 to 9 smaller than the Lp of layers 3 to 9.

It should be noted that the Lp values of part A of Table III are given as mean values ± SD which have been calculated from mean values of cell dimensions (diameter and length), dP/dV, $T_{1/2}$, and π^i according to Equation 2 without considering the propagation of errors in the different independently measured variables. Thus, the Gaussian law of error propagation has to be applied to evaluate the total error of a single measurement of Lp. This relation states that the error (such as the standard deviation, SD) of an indirectly determined parameter y (such as Lp) which is related to several directly measured independent quantities x_i [*i.e.* $y = f(x_1, x_2, x_3, \ldots x_n)$] will be given by (*e.g.* ref. 9):

$$SD_y = \pm \sqrt{\sum_{i=1}^{n} \left(\frac{\partial y}{\partial x_i}\right)^2 \cdot SD_{xi}^2}, \qquad (15)$$

where SD_y and SD_{xi} are the standard errors of y and the x_i and $\partial y/\partial x_i$ the partial derivatives of y with respect to the x_i.

Table III. *Hydraulic Parameters and Reflection Coefficients of Root Cells and of Entire Roots*

In (A), half-times of water exchange ($T_{½}$), the hydraulic conductivity (Lp), and dP/dV are given for hydrostatic experiments at the cell and root level. In (B), half times of osmotic responses of cells of different layers are given for two different osmotica (PEG 6000 and KCl) at osmotic concentrations ranging from 30 to 55 mOsmol (0.08–0.14 MPa osmotic pressure). The apparent reflection coefficients of part (C) refer to the same experiments as in (B). In (B) and (C), also $T_{r½}$ and σ_{sr} of entire roots are presented. All data are means of averages of individual cells or roots (n = number of cells or roots). The numbers of observations for individual cells were in (A) 3 to 5, and in (B) and (C) about 2. For individual entire roots, the number of observations were in (A) 3 to 5, and in (B) and (C) 4 to 16.

	Cortical Layers						Entire roots
	Rh	1st	2nd	3rd–4th	5–6th	7–9th	
(A) Hydraulic conductivity and elastic modulus of cortex cells (hydrostatic exp.)							
$T_{½}$ (s)	6.4 ± 1.9	7.9 ± 2.5	9.7 ± 2.8	2.2 ± 1.7	1.9 ± 0.6	2.7 ± 1.0	18 ± 6
$Lp \cdot 10^{7}$ ($m \cdot s^{-1} \cdot MP^{a-1}$)	3.4 ± 0.9	1.9 ± 0.6	3.5 ± 1.2	12.3 ± 7.9	14.5 ± 4.5	9.0 ± 3.4	1.6 ± 0.4
n	(14)	(25)	(22)	(20)	(13)	(10)	(52)
$dP/dV \cdot 10^{-13}$ ($MPa \cdot m^{-3}$)	3.3 ± 0.6	3.0 ± 1.4	1.2 ± 0.3	1.0 ± 0.2	1.1 ± 0.5	1.9 ± 0.4	—
n	(16)	(25)	(28)	(24)	(15)	(11)	
(B) Half-times of osmotic response in cortical layers ($T_{½}$)							$T_{r½}$ (s)
KCl	10 ± 4	28 ± 11	91 ± 18	72 ± 16	85 ± 8	107 ± 19	120 ± 25
n	(6)	(12)	(15)	(11)	(7)	(7)	(48)
PEG 6000	22 ± 7	42 ± 15	79 ± 21	76 ± 11	77 ± 14	103 ± 37	111 ± 21
n	(8)	(9)	(10)	(10)	(8)	(6)	(50)
(C) Apparent reflection coefficients of cortical cells (σ_s)							σ_{sr}
KCl	0.96 ± 0.08	0.88 ± 0.11	0.83 ± 0.10	0.80 ± 0.10	0.81 ± 0.14	0.76 ± 0.18	0.53 ± 0.06
n	(6)	(12)	(15)	(11)	(7)	(7)	(48)
PEG 6000	0.92 ± 0.11	0.78 ± 0.15	0.85 ± 0.09	0.82 ± 0.14	0.78 ± 0.16	0.81 ± 0.13	0.64 ± 0.04
n	(8)	(9)	(10)	(10)	(8)	(6)	(50)

Equation 15 assumes that the number of determinations for each of the independent variables is much larger than unity. This condition was fulfilled in the experiments of this paper. Using Equation 2 it is verified from Equation 15 that the relative error in Lp would be given by:

$$\frac{SD_{Lp}}{Lp} = \pm \sqrt{\left(\frac{\epsilon - \pi_i}{\epsilon + \pi_i}\frac{SD_d}{d}\right)^2 + \left(\frac{\epsilon}{\epsilon + \pi_i}\frac{SD_l}{l}\right)^2 + \left(\frac{\epsilon}{\epsilon + \pi_i}\frac{SD_{dP/dV}}{dP/dV}\right)^2 + \left(\frac{SD_{T1/2}}{T_{1/2}}\right)^2 + \left(\frac{SD\pi_i}{\epsilon + \pi_i}\right)^2}. \quad (16)$$

SD_{Lp} = standard deviation of Lp. Equation 16 incorporates errors due to all of the five independent variables (d, l, $T_{½}$, dP/dV, and π^i) which are used to determine Lp. From Table II, the error for the determination of the cell diameter and length will be 20 and 31%, respectively. The standard deviations in the determination of $T_{½}$ and dP/dV will be 25 and 10%, respectively (data not shown in Table III), and the error in the determination of π^i less than 0.03 MPa. Using these values and typical values of ϵ and π^i (ϵ = 2 MPa and of π^i = 0.6 MPa), the propagated error of Lp is calculated to be 37%. Thus, the propagated error in a single measurement is similar to the error due to the variation between cells which is given in Table III, A. If standard errors of the mean (SEM) are considered, the error in Lp is much smaller, because the standard deviations of the independent variables have to be divided by the square roots of the numbers of observations. By an analogous procedure, we get a relative error of the mean, *i.e.* SEM_{Lp}/Lp = 12.5%. It is evident from the calculation that the variation in cell dimensions (*i.e.* the cell surface area) contributes most to the total error, whereas the errors due to the measurements with the pressure probe are small (21).

Errors in the elastic modulus (ϵ) are similar to those in Lp, because Lp is less dependent on cell dimensions, but in addition depends on $T_{½}$. With the data of this paper, we get by error propagation a total error of 43% for the single measurement (SD) and 11% for the SEM. Again, the measurements of cell dimensions contribute most to the overall error whereas the measurements with the probe are fairly precise.

In the osmotic experiments (Table III, B), half times of the responses were similar to those obtained from hydrostatic experiments only for the rhizodermis. In all other cases, $T_{½}$ was much larger and strongly increased with increasing distance from the surface (see above). For cells in layers close to the endodermis, $T_{½}$ was similar to that of the entire root measured with the root pressure probe ($T_{r½}$). Within the limits of accuracy, there was no difference between the two different osmotica used (KCl and PEG 6000). Individual roots could be subjected to changes of the osmotic pressure by up to about 10 times during the duration of the experiments which lasted up to 12 h with a single root.

The data of reflection coefficients of cells (Table III, part C), indicate a value close to unity for the rhizodermis for nonpermeating solutes such as KCl and PEG 6000. There was a decrease in σ_s from the rhizodermis to the first cortical layer, but then σ_s was fairly constant within the cortex (F-test, KCl; F = 1.3; PEG 6000: F = 0.9; $p > 0.05$). With error propagation, the average of σ_s of cortex cells ± SD was calculated to be σ_s = 0.81 ± 0.17 and 0.80 ± 0.15 for KCl and PEG 6000, respectively. t-Tests showed that the difference of σ_s between the rhizodermis and the whole cortex was signifi-

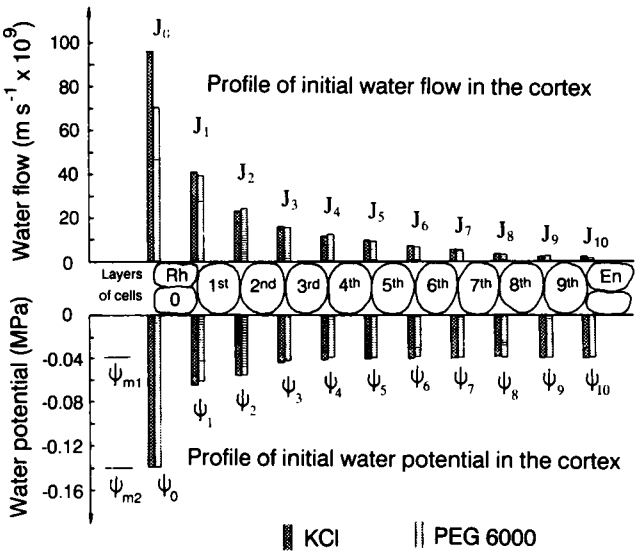

Figure 4. Profiles of initial water potential (ψ_j) and initial water flow (J_j) across the cortex calculated for a model root during osmotic dehydration using data from simultaneous determinations of hydraulic parameters at the root and cell levels (osmotica: KCl and PEG 6000). For the calculation, a change of the osmotic pressure of the root medium of 0.1 MPa was assumed. Values of J_j represent cumulative flows across individual cell layers in the cortex in $m^3 \cdot m^{-2} \cdot s^{-1}$ evaluated according Equation 7. ψ_j values represent the water potentials corresponding to the J_j (Eq. 10). ψ_{m2} = water potential of the solution during osmotic treatment (−0.14 MPa); ψ_{m1} = water potential of the original nutrient solution (−0.04 MPa); Rh = rhizodermis; En = endodermis.

cant for both osmotica ($p < 0.05$). However, the decrease from σ_s to σ_{sr} was significant either between the innermost cortical layer and entire roots or between the whole cortex and entire roots ($p < 0.0005$). For both, KCl and PEG 6000, σ_s values were not significantly different. However, the root σ_{sr} of PEG 6000 was significantly larger than that of KCl. This agrees with earlier findings on maize roots, where σ_{sr} of PEG 1000 was larger than that of NaCl and KNO_3 (20).

Calculation of Profiles of Water Flows and of Water Potential Across the Root

From the initial osmotic responses (osmotica: KCl and PEG 6000; osmotic pressure change: 0.1 MPa), the profiles of water flow (per m^2 of the surface area of the layer within the cortex) were calculated using Equation 9 (Fig. 4). It should be noted that the flows shown in the figure are cumulative flows (see Equation 7). Since the initial flows $[(dV/dt)_{t=0}$; Equation (8)] were fairly small for cells sitting deeper than in the second layer of the cortex, the contributions from the stele and xylem were rather small. Most of the water flowing out of the root was from the rhizodermis and the first layer of the cortex (70–80%). Since the half time of the response of the rhizodermis cell was faster for KCl than for PEG 6000, the contribution of the outermost layers to the overall flow was larger for KCl than for PEG. The resulting profile of initial water potential is given in Figure 4. In layers deeper than the second, the forces driving the flows ($\Delta\psi_j$) were rather small, and most of the potential dropped in the outermost layers. For the rhizodermis and for layers 1 and 2 of the cortex, the hydraulic conductivity of the cell wall material (Table IV) was estimated from Equations 11 and 10 and from the profiles of J_j and ψ_j to be in the range of 0.3 to $6.1 \cdot 10^{-9}$ $m^2 \cdot s^{-1} \cdot MPa^{-1}$. However, for deeper layers, it was not possible to estimate Lp_{cw} as above, because the errors in the initial values of ψ would have been relatively large. For these layers, the average value of Lp_{cw} from Table IV ($2.3 \cdot 10^{-9}$ $m^2 \cdot s^{-1} \cdot MPa^{-1}$) was used for the calculation of L_j from Equation 11. With the L_j of cortex layers and of the rhizodermis, the contribution of the apoplasmic and cell-to-cell path to L_j were calculated from Equations 11 and 12 (Table V). According to the cross- and longitudinal sections of the roots (see "Materials and Methods"), a mean cross-sectional area of the apoplast of γ_{cw} = 0.03 was assumed for the cells of the rhizodermis and a γ_{cw} = 0.02 for the cortex, respectively. The figures in Table V show that in all layers the contribution of the cell-to-cell path to overall water flow was much smaller than that of the apoplasmic path. However, the contribution of the cell-to-cell path varied considerably in the cortex (from 2–23%) because of the increase of cell Lp toward the stele (Table V).

DISCUSSION

In the research described in this paper, simultaneous determinations of water relation parameters at the root and cell level have been realized for the first time by a double pressure probe technique. The experiments allowed to estimate the contribution of different pathways (cell-to-cell and apoplasmic) to the overall radial water flow. The determination was only possible for osmotic experiments because of difficulties in obtaining the small and transient responses in turgor of cells when the root was experiencing changes of the hydrostatic pressure of the xylem. This is because the amounts of water dissipated from the xylem across the root were very small.

The model used to evaluate water flows across the cortical layers of maize roots was based on measurements of the rates of the initial shrinking of individual cells following an osmotic treatment. These measurements are possible with the cell pressure probe because changes of turgor pressure can be directly converted into changes of cell volume with high precision. The cumulative approach of calculating the flows neglected contributions from the apoplast and from internal parts of the roots (stele, xylem). This was justified because the comparison of the rates of initial shrinking of these parts with

Table IV. *Hydraulic Conductivity of Cell Walls, Lp_{cw} (m^2 s^{-1} MPa^{-1})*

Estimates of Lp_{cw} have been calculated from Equations 11 and 10 using the data of J_j and ψ_j from the profiles of initial water flow and water potential of osmotic experiment (Fig. 4) and from measured values of Lp. A mean cross-sectional area of 3% was assumed for cell walls of the rhizodermis and 2% for those of the cortex cells.

	Cortical Cell Layer		
	Rh	1st	2nd
$Lp_{cw} \cdot 10^9$ (KCl)	0.25	3.5	1.7
$Lp_{cw} \cdot 10^9$ (PEG 6000)	0.45	6.1	1.6

Table V. *Contribution of the Apoplasmic and Cell-to-Cell Path to the Overall Hydraulic Conductivities of Different Cell Layers of the Root Cortex (L_j in m s^{-1} MPa^{-1})*

For the first three cell layers L_j was calculated from values of initial water flow (J_j) and potential (ψ_j) according to Equation 10. For deeper layers, L_j was calculated from Equation 10 using a mean value of the data of Lp_{cw} given in Table IV. Numbers in brackets denote the percentage of the contribution of the parallel pathways to the overall value of L_j. γ_{cc} and γ_{cw} are the fractional contributions of the cell-to-cell and cell wall pathways to the total cross-sectional area (see Eq. 11).

	Rh	1st	2nd	3–4th	5–6th	7–9th
$L_j \cdot 10^7$	6.6	48.9	16.7	31.9	31	37.4
$\gamma_{cc} \cdot (Lp_i/2) \cdot 10^7$	1.6 (24%)	0.9 (2%)	1.7 (10%)	5.9 (18%)	7.0 (23%)	4.4 (12%)
$\gamma_{cw} \cdot (Lp_{cw}/d_{cj}) \cdot 10^7$	5.0 (76%)	48 (98%)	15 (90%)	26 (82%)	24 (77%)	33 (88%)

those of the cortex cells showed that the former were much smaller. The contribution of the apoplast should be fairly small as compared with the protoplasts (15). Thus, the values for the initial flows calculated from dP/dt at $t = 0$ are lower limits, although the contribution of internal parts may be only a few percent (Fig. 4). The determination of flows from the initial phase should also avoid most of the complications resulting from the diffusion of the osmotic solutes (KCl, PEG 6000) into the apoplast which may be important during later periods of time. The profiles calculated for the water potential and for the initial water flow show that both decline rapidly across the outermost layers and that during the initial period of time most of the water lost originates from the outermost layers. Initially, the water potential in the vacuoles (ψ_v) of tissue cells should still stay at the original level, and, hence, for the cells in the outermost layers there should be a significant water potential gradient across the cell membranes.

For technical reasons, data of the hydraulic conductivity of the cell wall material (Lp_{cw}) are hardly accessible. This is so because the apoplast of higher plant tissue cannot be separated from the protoplasts to measure its hydraulic conductivity. Thus, Lp_{cw} has to be determined by difference, *i.e.* by measuring the hydraulic conductivity of a tissue as well as that of the cell-to-cell path (protoplasts). The latter can be done by the conventional cell pressure probe, and the data of Lp incorporate both the symplasmic path (via plasmodesmata) and the transcellular (membrane-bound) path which can be also not separated to date. In the literature, there are only a few values of Lp_{cw} which have been mainly obtained on isolated cell walls of *Nitella*. They range between $Lp_{cw} = 0.5$ and $1.4 \cdot 10^{-10}$ $m^2 \cdot s^{-1} \cdot MPa^{-1}$ (for references see ref. 16). The values of Lp_{cw} estimated in this paper by the initial flow method are considerably larger than the values for *Nitella* and range between 0.3 and $6 \cdot 10^{-9}$ $m^2 \cdot s^{-1} \cdot MPa^{-1}$. The reason for the big difference is not known, but may be an inherent difference between algae and higher plants. Lp_{cw} may also depend on the species and on the type of tissue measured as well as on the growing conditions. A much larger value of Lp_{cw} than that found for the walls of young maize roots was measured for the hypocotyl of soybean using a pressure-perfusion technique ($8 \cdot 10^{-8}$ $m^2 \cdot s^{-1} \cdot MPa^{-1}$; 16). However, this high value should have been due to the involvement of transport via intercellular spaces which were filled with water during perfusion.

It can be seen from Equation 12 that the ratio of ρ would determine the relative contribution of water flowing either in the apoplasmic or in the cell-to-cell path. The data given in "Results" (Table V) show that for all layers the contribution of the apoplasmic path was larger than that of the cell-to-cell path due to the high value of Lp_{cw}. However, the rates varied because of the strong increase of Lp in the inner cell layers. Changes of Lp of cells of root tissue in radial direction have not yet been reported. The result is similar to that found earlier for the midrib tissue of maize leaves where the Lp of cells in the adaxial parts of the tissue was by an order of magnitude smaller than in the abaxial parts close to the peripheral vessels (23). For the leaf, this finding has been interpreted in terms of a better supply with water of parts further away from the vessels. Similarly, it may be possible that, in the root cortex, the increase of the hydraulic resistance of deeper layers (due to a reduction of surface area) may be compensated by an increase of Lp. As already mentioned in "Results", the measured Lp may also incorporate components from the vicinity of the protoplasts, *i.e.* from the apoplast and from adjacent protoplasts. However, these components should hardly play a role, since the amounts of water dissipated or taken up during a relaxation experiment are rather small (21) and the hydraulic conductivity of the cell wall is quite high. For example, using a value of $Lp_{cw} = 0.3$ to $6 \cdot 10^{-9}$ $m^2 \cdot s^{-1} \cdot MPa^{-1}$ (Table IV) and a wall thickness of 1 μm, the hydraulic conductivity of the cell wall (in the same units as Lp) would be 0.3 to $6 \cdot 10^{-3}$ $m \cdot s^{-1} \cdot MPa^{-1}$. This value is by 2 to 4 orders of magnitude larger than the measured Lp (Table III). Hence, the apoplast should play no role. This could change, if cell walls become suberised as it is found in the endodermis, but also in cells just below the rhizodermis in association with the formation of an exodermis (13). However, no exodermis could be detected in the young maize roots used in the experiments after staining with a berberine-aniline-blue fluorescent dye (1).

Another possibility which may affect the absolute value of cell Lp calculated from $T_{1/2}$ may result from anisotropic hydraulic properties of cortex cells, *i.e.* if Lp of a cell were different in radial, tangential, and longitudinal directions. This could be brought about by differences in the frequencies of plasmodesmata. However, there are, at present, no indications that such an anisotropism of Lp exists, and the question is rather speculative. Also, since the overall hydraulic conductivity of the membranes of higher plants is usually large, the contribution of plasmodesmata should be smaller than it is commonly thought.

The absolute value of Lp of the outer part of the cortex was

comparable to that given previously using the same technique for measuring Lp (20). The mean Lp measured in the inner part of the cortex was by a factor of 5 larger than that given previously. However, in the previous study the number of cells measured was much smaller and no effort was made to work out a possible dependence of Lp on the position and, therefore, the effect could have been overlooked.

As reported in earlier papers (6, 18, 20), the hydraulic conductivity of entire roots (Lp_r) measured in hydrostatic and osmotic experiments differed by a factor of 6 to 11. This has been explained by the fact that by using an osmotic driving force, the effective force in the apoplast should be rather small, because the reflection coefficient of the cell wall material should be low. Thus, in the osmotic experiments, the overall flow should have a substantial cell-to-cell component. This explanation does not contradict the finding of this paper that during the osmotic dehydration of the cortex most of the water flows around cells, because in the measurements with the root pressure probe the loss of water from the xylem into the medium across the entire barrier is considered. Hydrostatic gradients applied between xylem and medium cause a rapid flow around cells due to the high Lp_{cw}, whereas in the osmotic experiments this is not the case, because the gradient in the water potential (osmotic pressure) cannot propagate fast in the apoplast. There may be also some buffering effect due to the storage capacity of the cortex for water in the osmotic experiment, but this effect cannot completely explain the discrepancy, because the differences between osmotic and hydrostatic values of Lp_r have been also found under conditions of steady flow (18).

As in the cortical tissue, some apoplasmic by-pass should also occur in the endodermis as discussed previously (15, 18, 20). In the endodermis, the apoplasmic water permeability should depend on the developmental state of the root and on the species. For example, for roots of barley (*Hordeum distichon*) and bean (*Phaseolus coccineus*) no differences between osmotic and hydrostatic Lp_r have been found (17, 19), which may point to more tight Casparian bands. It should be noted that a significant by-pass of water and NaCl have been also reported for roots of cotton and rice, respectively (14, 24). In other cases, the Casparian band seemed to be fairly tight (*e.g.* ref. 7).

The low values of reflection coefficients of entire roots found in this paper are in line with earlier findings for maize and other species using the root pressure probe (17–20). They are also in line with findings from other labs using different techniques (5, 10). Low reflection coefficients for a composite structure such as the root may be explained in terms of the arrangement of different osmotic barriers in the root in series (different cell layers) and in parallel (apoplasmic and cell-to-cell pathways). Irreversible thermodynamics shows that the reflection coefficients of such composite barriers should be some kind of a weighted mean of the σ values of individual barriers which contribute to the overall value according to their solute permeability (series arrangement) or to their hydraulic conductivity (parallel arrangement) (for references, see ref. 20). In this way, low σ_{sr} values of roots are understandable, and a low σ_{sr} would not necessarily be correlated with a high solute (nutrient) leakage which would not allow a proper function of roots. Thus, the simple osmometer model of the root predicting some kind of an ideally semipermeable endodermis and a $\sigma_{sr} \approx 1$ has to be extended into a 'composite-membrane model of the root' (15, 17, 20).

The experiments of this paper support this view. The σ_s values measured for cells sitting right at the root surface were close to unity as one would expect for an isolated cell. However, in deeper layers, σ_s decreased, since the cell was surrounded by membrane-like layers exhibiting a σ substantially lower than unity. The effect increased towards the xylem, although within the limits of accuracy no changes could be found within the cortex. The effect resembles that of unstirred layers of increasing thickness, but is obviously different in nature because the measured ratio of $\Delta P/\Delta\pi^o$ (Eq. 3) was substantially smaller than unity for deeper cell layers even after waiting for solute equilibration for rather long periods of time. Osmoregulatory effects may contribute to the apparently low values of σ_s and σ_{sr}, but it is hard to envisage how they could completely explain the effects because water flow equilibration is usually much more rapid than changes in concentrations due to active flow (see computer simulation in ref. 17).

The results of this paper show that the double pressure probe technique seems to be an attractive tool for measuring flows of water in tissues and for evaluating models of water transport. The technique could be also used for tissues different from the root. It could be also applicable for the hydrostatic type of experiments provided that stationary rather than transient gradients can be set up. In the double pressure probe technique, also the transient changes in turgor pressure of cells and their dependence on the position in the tissue could be used to evaluate the hydraulic data used to model the radial transport of water and solutes across the root cylinder. This type of an evaluation of the propagation of changes of water potential in root tissue will be dealt with in a subsequent paper (E Steudle, GL Zhu, unpublished data).

ACKNOWLEDGMENTS

The authors are indebted to Dr. Carol A. Peterson, Department of Biology, University of Waterloo, Ontario, Canada, for her help in the anatomic studies, and to Dr. U. Lüttge, Institut für Botanik, Technische Hochschule, Darmstadt, FRG, for discussing the work. We also thank Mr. B. Stumpf, University Bayreuth, for expert technical assistance.

LITERATURE CITED

1. **Brundrett MC, Enstone DE, Peterson CA** (1988) A berberine aniline blue fluorescent staining procedure for suberin, lignin, and callose in plant tissues. Protoplasma **146:** 133–142
2. **Clarkson DT, Robards AW, Stephens JE, Stark M** (1987) Suberin lamellae in the hypodermis of maize (*Zea mays*) roots; development and factors affecting the permeability of hypodermal layers. Plant Cell Environ **10:** 83–93
3. **Dainty J** (1985) Water transport through the root. Acta Hortic **171:** 21–23
4. **Fiscus EL** (1975) The interaction between osmotic and pressure induced water flow in plant roots. Plant Physiol **55:** 917–922
5. **Fiscus EL** (1977) Determination of hydraulic and osmotic properties of soybean root systems. Plant Physiol **59:** 1013–1020
6. **Frensch J, Steudle E** (1989) Axial and radial hydraulic resistance to roots of maize (*Zea mays* L.). Plant Physiol **91:** 719–726
7. **Hanson PJ, Sucoff EI, Markhart AH** (1985) Quantifying apoplastic flux through red pine root systems using trisodium, 3-hydroxy-5,8,10-pyrenetrisulfonate. Plant Physiol **77:** 21–24

8. **Hüsken D, Steudle E, Zimmermann U** (1978) Pressure probe technique for measuring water relations of cells in higher plants. Plant Physiol **61:** 158–163
9. **Kreyszig E** (1973) Statistische Methoden und ihre Anwendungen. Vandenhoeck & Ruprecht, Göttingen.
10. **Miller DM** (1985) Studies of root function in *Zea mays*. III. Xylem sap composition at maximum root pressure provides evidence of active transport into the xylem and a measurement of the reflection coefficient of the root. Plant Physiol **77:** 162–167
11. **Newman EI** (1976) Interaction between osmotic- and pressure-induced water flow in plant roots. Plant Physiol **57:** 738–739
12. **Passioura JB** (1988) Water transport in and to roots. Annu Rev Plant Physiol Plant Mol Biol **39:** 245–265
13. **Peterson CA** (1988) Exodermal Casparian bands: their significance for ion uptake by roots. Physiol Plant **72:** 204–208
14. **Radin J, Matthews M** (1989) Water transport properties of cortical cells in roots of nitrogen- and phosphorus-deficient cotton seedlings. Plant Physiol **89:** 264–268
15. **Steudle E** (1989) Water flow in plants and its coupling to other processes: an overview. *In* S Fleischer, B Fleischer, eds, Methods in Enzymology, Vol 174, Biomembranes, Part U: Cellular and Subcellular Transport: Eukaryotic (Nonepithelial) Cells. Academic Press, New York, pp 183–225
16. **Steudle E, Boyer JS** (1985) Hydraulic resistance to radial water flow in growing hypocotyl of soybean measured by a new pressure-perfusion technique. Planta **164:** 189–200
17. **Steudle E, Brinckmann E** (1989) The osmometer model of the root: water and solute relations of roots of *Phaseolus coccineus*. Bot Acta **102:** 85–95
18. **Steudle E, Frensch J** (1989) Osmotic responses of maize roots. Water and solute relations. Planta **177:** 281–295
19. **Steudle E, Jeschke WD** (1983) Water transport in barley roots. Measurements of root pressure and hydraulic conductivity of roots in parallel with turgor and hydraulic conductivity of root cells. Planta **158:** 237–248
20. **Steudle E, Oren R, Schulze ED** (1987) Water transport in maize roots. Measurement of hydraulic conductivity, solute permeability, and of reflection coefficients of excised roots using the root pressure probe. Plant Physiol **84:** 1220–1232
21. **Steudle E, Smith JAC, Lüttge U** (1980) Water relation parameters of individual mesophyll cells of the CAM plant *Kalanchoe daigremontiana*. Plant Physiol **66:** 1155–1163
22. **Taura T, Iwaikawa Y, Furumoto M, Katou K** (1988) A model for radial water transport across plant roots. Protoplasma **144:** 170–179
23. **Westgate ME, Steudle E** (1985) Water transport in the midrib tissue of maize leaves. Direct measurement of the propagation of changes in cell turgor across a plant tissue. Plant Physiol **78:** 183–191
24. **Yeo AR, Yeo ME, Flowers TJ** (1987) The contribution of an apoplastic pathway to sodium uptake by rice roots in saline conditions. J Exp Bot **38:** 1141–1153